Modeling the Argasid Tick (*Ornithodoros moubata*) Life Cycle

Sara M. Clifton, Courtney L. Davis, Samantha Erwin, Gabriela Hamerlinck, Amy Veprauskas, Yangyang Wang, Wenjing Zhang, and Holly Gaff

Abstract The first mathematical models for an argasid tick are developed to explore the dynamics and identify knowledge gaps of these poorly studied ticks. These models focus on *Ornithodoros moubata*, an important tick species throughout Africa and Europe. *Ornithodoros moubata* is a known vector for African swine fever (ASF), a catastrophically fatal disease for domesticated pigs in Africa and Europe. In the absence of any previous models for soft-bodied ticks, we propose two mathematical models of the life cycle of *O. moubata*. One is a continuous-time differential equation model that simplifies the tick life cycle to two stages, and the second is a discrete-time difference equation model that uses four stages. Both models use two host types: small hosts and large hosts, and both models find that either host type alone could support the tick population and that the final tick density is a function of host density. While both models predict similar tick equilibrium values, we observe significant differences in the time to equilibrium. The results

S. M. Clifton
Department of Mathematics, University of Illinois at Urbana-Champaign, Urbana, IL, USA

C. L. Davis
Natural Science Division, Pepperdine University, Malibu, CA, USA

S. Erwin
Department of Population Health and Pathobiology, College of Veterinary Medicine, North Carolina State University, Raleigh, NC, USA

G. Hamerlinck
BioQUEST Curriculum Consortium, Inc., Madison, WI, USA

A. Veprauskas
Mathematics Department, University of Louisiana at Lafayette, Lafayette, LA, USA

Y. Wang
Mathematical Biosciences Institute, Ohio State University, Columbus, OH, USA

W. Zhang
Department of Mathematics and Statistics, Texas Tech University, Lubbock, TX, USA

H. Gaff (✉)
Department of Biological Sciences, Old Dominion University, Norfolk, VA, USA

A. Radunskaya et al. (eds.), *Understanding Complex Biological Systems with Mathematics*, Association for Women in Mathematics Series 14,
https://doi.org/10.1007/978-3-319-98083-6_4

demonstrate the likely establishment of these ticks if introduced into a new area even if there is only one type of host. These models provide the basis for developing future models that include disease states to explore infection dynamics and possible management of ASF.

1 Introduction

Unlike the well-studied hard-bodied (ixodid) ticks, soft-bodied (argasid) ticks exist in relative obscurity. Perhaps due to the argasid tick's comparatively complex life cycle and its (as yet) limited impact on human health, no species of soft-bodied tick has been mathematically modeled. In contrast, the life histories and population dynamics of ixodid ticks, the vectors for diseases such as Rocky Mountain spotted fever and Lyme disease, have been characterized quantitatively [13, 14]. This void is not trivial; soft-bodied ticks such as *Ornithodoros moubata* are vectors of devastating human and animal diseases including African swine fever (ASF) in domesticated pigs [16, 37] and African relapsing fever in humans [11]. ASF and its vector *O. moubata* are of particular concern because, although the disease has thus far only emerged in Africa and Europe, global spread seems inevitable [9]. ASF is especially difficult to eradicate due to the absence of available vaccines, multiple wild reservoirs, and limited knowledge of the vector's complex life cycle [31].

Like many argasid tick species [18], *O. moubata* are opportunistic feeders. The ticks typically inhabit warthog burrows and feed on animals that also occupy the burrows, such as warthogs, mice, rats, and mongooses [17, 30]. Ticks and wild suids infected with the ASF virus experience minimal physiological effects and therefore serve as natural reservoirs for the virus [4]. However, when domesticated pigs become infected with the virus through contact with infected objects, ticks, or other infected pigs or wild suids, the disease can kill an entire livestock herd in a matter of days [6, 35]. Given that no vaccines are available, farmers typically impose a strict quarantine of unaffected pigs and culling of exposed pigs [24, 29]. Since *O. moubata* are capable of surviving extended periods of time without blood meals, this management strategy may be ineffective due to the infeasibility of removing smaller hosts (i.e., mice or mongooses) from the affected area for prolonged periods of time. Therefore, it is imperative to quantitatively understand the complex life cycle of this tick. By modeling soft ticks, we aim to better understand what drives soft tick population expansion in order to control the spread of both the ticks and the diseases they carry.

This paper develops two exploratory mathematical models to capture the dynamics of the argasid tick. Using *O. moubata* as the motivation, both a discrete-time and continuous-time model are developed. We incorporate features of the unique life history of soft ticks, including the effects of host type on life history events that depend on blood meals, such as reproduction. Specifically, our models use two generic host types: a large host representing suids such as warthogs or domestic swine, and a less beneficial small host, such as mongooses or other small mammals.

Since current ASF control strategies involve removing swine from the affected area for several years [29], in future work this type of model formulation will allow us to examine the effectiveness of this strategy on disease eradication.

We first introduce a continuous-time model of tick and host dynamics that reduces the complex system to two stages, which allows us to analytically examine how tick population dynamics are impacted by host type. This model serves as a minimal mathematical model of argasid tick dynamics. With limited field data, we produce qualitative and (limited) quantitative predictions for tick growth with two host types. We then present a discrete-time model of tick and host dynamics that enables us to track multiple nymph life stages and examine the effects of circumventing late nymph stages following a sufficient blood meal from a large host. This model captures more unique features of the argasid tick life cycle, and therefore it requires more field data to produce quantitative predictions.

2 *Ornithodoros moubata* Biology

Argasid ticks have a complex and variable life history. Unlike ixodid ticks, who have a strict three-stage life history [36], *O. moubata* may progress through up to six nymphal stages before molting to their adult life stage [1]. Figure 1 shows the

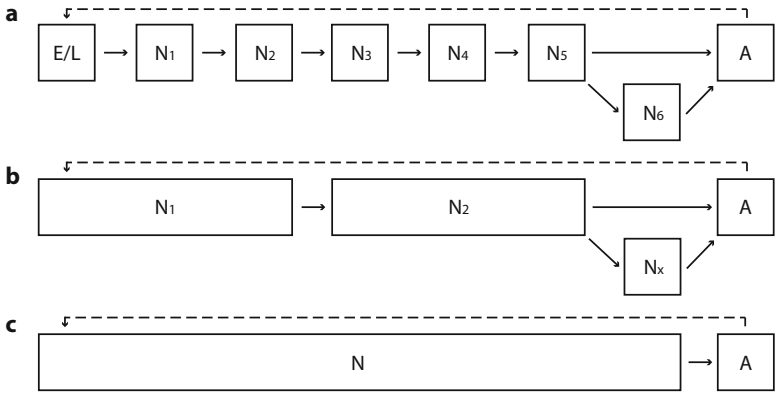

Fig. 1 Life cycle of *O. moubata*. (**a**) The full life cycle of *O. moubata* includes the egg and larval stage (E/L), then a variable number of instars (N_i) based on quality and quantity of blood meals, and finally the adult stage (A). (**b**) The discrete-time model simplifies the *O. moubata* life history to four life stages. The first nymphal stage, N_1, represents the summation of the egg/larval stage plus the first two instars. The second nymphal stage, N_2, includes the biological instars three through five. Individuals may transition out of stage N_2 by molting into an adult, A, given a sufficient blood meal. Insufficient blood meals result in molting to an additional nymphal instar, N_x. Adults, A, then reproduce and the females lay eggs. (**c**) The continuous-time model simplifies the *O. moubata* life history traits even more by combining all immature stages in one class, N. Immature individuals either remain as nymphs or move to the adult stage, A, depending on timing and the sufficiency of blood meal

complete life history of *O. moubata* (Fig. 1a) and the mathematical simplifications made for the discrete-time (Fig. 1b) and continuous-time (Fig. 1c) models presented in this paper. Eggs hatch to their larval stage then molt into the first nymph stage without completing a blood meal, and then advance through the nymph stages and to the final adult stage upon successful completion of a blood meal at each stage [23]. When an individual reaches a fifth nymphal stage, it has the ability to transition to its adult stage but must complete a large, high quality blood meal to do so. If that blood meal is either small or low quality, the nymph may delay its adult molt and instead transition to a sixth nymph stage [25, 26].

A single adult female can lay up to three clutches in her lifetime [17]. Clutch size is dependent on the quality of the blood meal consumed by the adult female before oviposition. While *O. moubata* do not appear to exhibit a host preference when feeding, significant differences in clutch size have been observed when adult ticks feed on different hosts. Female *O. moubata* have been shown to produce 500 eggs per clutch when fed on warthogs and between 100 and 200 eggs per clutch when fed on small hosts [3, 5, 25].

All blood meals taken by *O. moubata* are completed within an hour, and each meal can come from a different individual of unique host species [17]. A blood meal can be interrupted by the host (i.e., the host scratches at the tick or moves, causing the tick to detach) (A. Bastos, pers. comm.). During feeding, *O. moubata*, like all argasid ticks, excretes excess fluid during blood meals rather than returning fluids to the host, potentially causing host death by exsanguination [2].

Their extremely long lifespan adds to the complexity of the *O. moubata* life cycle. In a laboratory setting, *O. moubata* has been shown to complete its life cycle in a minimum of 76 days, completing each nymph stage in approximately 2 weeks, but to have a potential lifespan of 18 years [23]. In particular, an adult tick can survive up to 5 years without feeding while each nymph stage can survive up to 2 years without feeding [17].

The differences in life history events (i.e., the seemingly optional sixth nymph stage) depend on host type, suggesting that we must consider the availability of various hosts in order to understand the dynamics of an *O. moubata* population. In addition to host considerations, difficulties in modeling population dynamics of the *O. moubata* system come from the immense biological complexity of the soft tick life history and the general lack of empirical data. Parameters are estimated from literature and expert opinion to provide ranges for sensitivity analyses of both models. The results of both models are compared; specifically, we compare the total tick density at equilibrium, the time to reach equilibrium, the average tick population growth rate, and the net reproductive number R_0. This work provides the foundation for future models to include swine fever dynamics and control.

3 Parameter Selection

Parameter values are estimated from published literature when available. For parameters for which there is no published information, we explore a range of potential values to help identify key parameters to investigate with future biological research.

We approximate the small host parameter values with empirical data from small mammals known to be utilized by *O. moubata* (e.g., mice, mongooses). These small hosts are likely to inhabit unoccupied warthog burrows and will frequently come into contact with *O. moubata* (A. Bastos, pers. comm.). All large host parameter values are approximated with data from wild suids, the optimal reservoir hosts for *O. moubata* [17]. To estimate the carrying capacity of hosts for our model, we extrapolate from the densities of wild African populations of mongooses and mice as representatives of small hosts and of wild African suid populations for the optimal large host. The range of mongoose (*Suricata suricatta*) density in the southern Kalahari is reported to be 32–95 animals per hectare [8]. The density of the striped mouse (*Rhabdomys pumilio*) was found in moderate to high quality habitat to be 20–73.3 mice per hectare [33]. Following these values as representatives of small hosts for our model, we assume that the range in carrying capacity of the environment for small hosts is 10^{-2} to 50 animals per hectare. We have chosen to use 10^{-2} to 10 animals per hectare for the carrying capacity of our large hosts following the reported warthog density in Kruger National Park [22].

Similarly, to define ranges for the net growth rate of hosts for our model, we extrapolate from the average birth rates of small and large hosts. Mongoose populations have, on average, four litters a year with 2.4 pups per litter [8]. The striped mouse has been shown to have two litters per year of 5.3 pups on average [32] Therefore, these small hosts will each have approximately 10^{-2} pups per week per individual. We ignore all seasonal or phenological variation in host dynamics and assume these rates are constant throughout the year. The net growth rate of the large hosts is similar to that of the small hosts. The reproductive potential of a warthog population (*Phacochoerus aethiopicus* in the Eastern Selous Game Reserve, Tanzania) was estimated to be 2.6 hoglets per year per female [7], or approximately 10^{-2} hoglets per week per individual, which we have used as a lower bound.

Progression through the *O. moubata* life cycle as well as reproduction depends on obtaining blood meals. We define the maximal sustainable tick population on small and large hosts to be the amount of blood loss that can occur with no deleterious effects on the host organism. We have estimated this range for small and large hosts to be 1–200 and 400–600 ticks, respectively. There is minimal variation in weight for blood meals taken from a range of small hosts [25], suggesting that all blood meals are approximately the same size across all small hosts. As warthogs, the large host, are significantly larger than any of our small hosts, they will have more blood meals to give before experiencing any negative effects related to blood loss. While density-dependent population regulation has not been successfully quantified for

argasid ticks [15], we include this as a competitive interaction for a finite number of shared hosts available to immature and adult tick populations.

Adult female *O. moubata* have been shown to lay clutches of 100–200 eggs when fed on suboptimal hosts and up for 500 eggs when fed on warthogs, the optimal host [3, 5, 25]. As these clutch sizes were observed in an optimal laboratory setting, we increase the parameter range for tick birth rates to better approximate natural populations. The ticks are subjected to constant density-independent death rates that are determined solely by age as well as density-dependent death rates that reflects natural death from age and other environmental risks such as predation. Although blood meals from large hosts tend to be larger and result in slower digestion, which may reduce molting rates, the quality of the blood meal has also been shown to have a significant impact on molting rates [25, 26]. Because it is difficult to obtain molting rates for ticks feeding on large hosts, little data are available on these rates. The two models presented in this paper make different assumptions on the molting rates, which are discussed when the models are introduced.

4 Continuous-Time Model

We extend a continuous-time population-level model for hard-bodied (ixodid) ticks [14] to soft-bodied (argasid) ticks. The hard-bodied tick model considers a host population that grows logistically and a tick population that grows logistically with a host-dependent carrying capacity. Since the soft-bodied tick has a more complex life history (e.g., host-dependent life stages), we add a second class of host and a second tick life stage. The tick of motivating interest, *O. moubata*, has many more life stages, but we ignore that complexity for now in the continuous-time model.

We consider a set of host populations with small and large mammals (e.g., rodents and swine). Both populations grow logistically and independently of each other:

$$\frac{\mathrm{d}S}{\mathrm{d}t} = r_S \left(1 - \frac{S}{K_S}\right) S, \tag{4.1}$$

$$\frac{\mathrm{d}L}{\mathrm{d}t} = r_L \left(1 - \frac{L}{K_L}\right) L, \tag{4.2}$$

where S and L are the densities of small and large hosts, respectively, K_S and K_L are the carrying capacities per area of the small and large hosts, and r_S and r_L are the net growth rates of small and large hosts. Table 1 summarizes the host parameters and estimated values.

We consider a population of ticks with two major life stages (female nymphs and female adults), where N and A are the densities of nymph and adult ticks, respectively. Adult ticks lay large clutches of eggs at a rate b_L if they feed on large (ideal) hosts and lay small clutches of eggs at a rate b_S if they feed on small (non-ideal) hosts. In other words, new nymphs are born when adult ticks and hosts interact via a blood meal.

Table 1 Variables and parameters for the host populations for the continuous-time model

Term	Meaning	Units	Range	Baseline	Citation(s)
S	Density of small mammal hosts	[1/ha]	–	–	–
L	Density of large mammal hosts	[1/ha]	–	–	–
K_S	Carrying capacity for small hosts per area	[1/ha]	$(10^{-2}, 50)$	1	[8, 33]
K_L	Carrying capacity for large hosts per area	[1/ha]	$(10^{-2}, 10)$	0.025	[22]
r_S	Net growth rate for small hosts	[1/week]	$(10^{-2}, 5)$	0.1	[8, 32]
r_L	Net growth rate for large hosts	[1/week]	$(10^{-3}, 10^{-1})$	0.03	[7]

Area is measured in hectares ($100\,\mathrm{m}^2$); time is measured in weeks

We assume large hosts can feed M_L ticks and small hosts can feed M_S ticks without significant ill effects due to blood loss. Therefore, the number of meals available for ticks is $M_S S + M_L L$. Because nymphs and adults compete among each other for this limited food resource, competition both within and between the tick stages is included. We model the competition as an age-structured competitive Lotka–Volterra system [20], where c_N and c_A are the total competitive death rates for nymphs and adult ticks, and α_N and α_A are the relative competition weights for nymphs and adults.

Additionally, nymphs molt into adult ticks after a sufficient blood meal from a small or large hosts at rate γ_S or γ_L, respectively. In other words, new adults are "born" when nymphs interact with hosts via a blood meal. Here we assume equal molting rates for both host species. Finally, each life stage has its own death rate: d_N for nymphs and d_A for adults. The system describing these dynamics is given by:

$$\frac{\mathrm{d}N}{\mathrm{d}t} = \underbrace{(b_S S + b_L L)A}_{\text{birth}} - \underbrace{\frac{c_N}{M_S S + M_L L}(N + \alpha_N A)N}_{\text{competition}} - \underbrace{d_N N}_{\text{death}} - \underbrace{(\gamma_S S + \gamma_L L)N}_{\text{molting}}, \tag{4.3}$$

$$\frac{\mathrm{d}A}{\mathrm{d}t} = \underbrace{(\gamma_S S + \gamma_L L)N}_{\text{molting}} - \underbrace{\frac{c_A}{M_S S + M_L L}(\alpha_A N + A)A}_{\text{competition}} - \underbrace{d_A A}_{\text{death}}. \tag{4.4}$$

Refer to Fig. 1c for a schematic of model (4.1)–(4.4). Table 2 summarizes the tick parameters and estimated values.

4.1 Numerical Results

We investigate the continuous-time tick-only model (4.3) and (4.4) for constant host populations through an analytical approach in Appendix. Because the two host populations converge to stable steady states in the long run, we assume populations

Table 2 Variables and parameters for the tick population for the continuous-time model

Term	Meaning	Units	Range	Baseline	Citation(s)
N	Density of nymph ticks	[1/ha]	–	–	
A	Density of adult ticks	[1/ha]	–	–	
M_S	Maximum sustainable ticks per small host	Unitless	$(1,\ 200)$	100	Estimated
M_L	Maximum sustainable ticks per large host	Unitless	$(400,\ 600)$	500	Estimated
b_S	Birth rate for ticks due to small host meal	[ha/week]	$(10^{-2}, 5)$	0.7	[3, 5, 25]
b_L	Birth rate for ticks due to large host meal	[ha/week]	$(0.1,\ 15)$	4.0	[3, 25]
d_N	Density-independent death rate for nymph ticks	[1/week]	$(10^{-3},\ 10^{-1})$	0.01	[17]
d_A	Density-independent death rate for adult ticks	[1/week]	$(10^{-3},\ 10^{-1})$	0.004	[17]
γ_S	Molting rate given small host meal	[ha/week]	$(0.02,\ 1)$	0.5	[23]
γ_L	Molting rate given large host meal	[ha/week]	$(0.02,\ 1)$	0.5	[23]
c_N	Total competitive (density-dependent) death rate for nymph ticks	[1/week]	$(10^{-3},\ 10^{-1})$	0.005	Estimated
c_A	Total competitive (density-dependent) death rate for adult ticks	[1/week]	$(10^{-3},\ 10^{-1})$	0.002	Estimated
α_N	Relative competition for nymph from adults	Unitless	$(10^{-1},\ 100)$	1	Estimated
α_A	Relative competition for adults from nymph	Unitless	$(10^{-1},\ 100)$	1	Estimated

Area is measured in hectares ($100\,m^2$); time is measured in weeks

of large and small hosts are constant and prove populations of nymph and adult ticks are non-negative and bounded if their initial states are non-negative. We find that tick persistence depends on the threshold value (the net reproductive number)

$$R_0(S, L) = \frac{(L\gamma_L + S\gamma_S)}{(d_N + L\gamma_L + S\gamma_S)} \frac{(Lb_L + Sb_S)}{d_A}. \tag{4.5}$$

We note that, since we are assuming the host populations are at carrying capacity, S and L can be replaced by K_S and K_L. The value R_0 has the interpretation of the average number of offspring produced by a nymph in its lifetime, where the first factor of R_0 is the probability of a nymph reaching the adult stage and the second factor gives the average number of offspring produced by an adult in its lifetime.

When $R_0 < 1$, the tick-free steady state (equilibrium solution) $E_0 = (0, 0)$ is locally asymptotically stable. When $R_0 > 1$, E_0 loses its stability, and a positive steady state for the tick population, E_1, emerges and is locally asymptotically stable. We further prove that E_1 does not admit a Hopf bifurcation. This result agrees with the numerical simulation results, which show no oscillation in the tick model (4.3) and (4.4). The details of the proofs are in Appendix.

We use the continuous-time tick system (4.1)–(4.4) and the parameters outlined in Tables 1 and 2 to numerically simulate scenarios that represent the soft-bodied

tick population. Here, we are motivated by scenarios that may be observed when dealing with the spread of ASF. Specifically, when ASF is detected in a pig farm, the domesticated swine (large hosts) are removed, but it is unfeasible to eliminate the small hosts. Therefore, we consider two scenarios. For both, we assume that there is no way to regulate the small host density, and therefore, small hosts are at carrying capacity. For the first scenario, we assume that no large hosts are present, as may occur if the domesticated pigs are removed. In the second case, large hosts are introduced at a low level and are then allowed to increase to carrying capacity, as may be observed when the domesticated pigs are reintroduced. Comparing these scenarios allows us to examine how much larger the tick density becomes when large hosts are present. In both scenarios, we assume that initially there are 70 nymphs present and no adults. As this number is the (female) clutch size for an adult tick feeding on a small host, we choose this initial condition to represent the case where ticks are introduced to an area due to a female tick arriving to the area (likely through transportation on a host) and laying a clutch. By examining the time to equilibrium, this allows us to examine how quickly the tick population may grow if introduced to a region, which may also be important for managing ASF.

For our simulation we use Matlab 2017 and the built-in ODE solver, ode23. We use the baseline parameters listed in Tables 1 and 2 and the initial conditions S(0)=1 small host per hectare, L(0) = 0 (Fig. 2a) or L(0) = 0.01 (Fig. 2b) large hosts per hectare, N(0)=70 nymph ticks per hectare, and A(0)=0 adult ticks per hectare. We solve (4.1)–(4.4) numerically and find that within 2 years the populations are at a steady state, as given in Table 3. In Fig. 2 we see there are approximately twice as many adult ticks as nymph ticks. It is also noteworthy that once the host population is stable, there is no change in the tick population size.

By modeling soft ticks, we aim to better understand what drives the soft tick population and how to mitigate their potential expansion into new areas. In Fig. 3, we show how the equilibrium total tick density is affected by host density. In Fig. 3a, we investigate the tick dynamics with one host and change the host carrying capacity. We consider the case where there are no small hosts and increase the large host density from 0.01 to 10 per hectare, based on the ranges in Table 1. We find that the total tick equilibrium increases linearly to 2×10^6 per hectare.

Similarly, we test the case in which there are no large hosts and increase the small hosts equilibrium from 0.01 to 50 per hectare, based on the ranges in Table 1. We find that the total tick equilibrium increases approximately linearly to 7.5×10^5 per hectare. In Fig. 3b, we vary both the large and small host equilibrium. We find that if both host populations are small, the tick population will die out. However, as either host population is increased, the total tick population equilibrium increases.

4.2 Identifiability and Sensitivity Analysis

Because many of the parameters for model (4.1)–(4.4) are not currently known, we consider a wide range of plausible parameters (shown in Tables 1 and 2). Given

Table 3 A comparison of the continuous-time and discrete-time model outputs for two different initial host densities when the tick population initially has 70 (first-stage) nymphs

		Initial host density	
		$S(0) = 1, L(0) = 0$	$S(0) = 1, L(0) = 0.01$
Continuous model	Eq. size	14,165 ticks/ha	17,330 ticks/ha
	Eq. time	35.1 weeks	114 weeks
	Avg. eq. time	0.002 weeks/(tick/ha)	0.007 weeks/(tick/ha)
	Avg. growth rate	417 ticks/ha/week	153.85 ticks/ha/week
	R_0	171.6 ticks/ha	196.2 ticks/ha
Discrete-time model	Eq. size	8600 ticks/ha	11, 226 ticks/ha
	Eq. time	468.7 weeks	474.7 weeks
	Avg. eq. time	0.054 weeks/(ticks/ha)	0.042 weeks/(ticks/ha)
	Avg. growth rate	18.4 ticks/ha/week	23.6 ticks/ha/week
	R_0	198.1 ticks/ha	248.9 ticks/ha

Equilibrium time is calculated as the time it takes the tick population density to reach within 1% of the equilibrium tick density. Average equilibrium time is calculated as the time to equilibrium divided by the equilibrium tick density. Average growth rate is calculated as 1/(average equilibrium time) and is defined as the total tick density increase at equilibrium divided by the time for the population to reach 99% of the equilibrium. R_0 is calculated by Eqs. (4.5) and (5.6) for the continuous-time and discrete-time model, respectively, when present host populations are at carrying capacity

time series data of the number of ticks and a constant number of hosts, the model parameters are structurally identifiable, although some are only identifiable in sets. Using the web application COMBOS [28], we find that c_N, c_A, d_N, d_A, α_N, and α_A are uniquely identifiable parameters, and $b_L K_L + b_S K_S$, and $K_L \gamma_L + K_S \gamma_S$ are uniquely identifiable parameter sets. For this analysis to be tractable, we must know the total blood meals available to the ticks ($M_S K_S + M_L K_L$).

To understand the sensitivity of the equilibrium tick densities to the parameters chosen, we perform a global sensitivity analysis. This is done with Latin hypercube sampling (LHS) and partial rank correlation coefficients (PRCC) [27]. A total of 1000 simulations are executed. The parameter ranges are listed in Tables 1 and 2, and parameter values are sampled from a uniform distribution, see Fig. 4a.

The sensitivity analysis reveals that total tick density at equilibrium is significantly ($p < 0.001$) and positively correlated with the large and small host carrying capacities, K_L and K_S, and the tick birth rates due to large and small host blood meals, b_L and b_S. As such, if the environment can sustain more hosts, then we will see an increase in the total tick density. Moreover, if the birth rate of ticks after a host meal increases, then we will see an increase in the total tick density. In addition, the simulations reveal that the competition parameters α_N, α_A, c_N, and c_A have a significant ($p < 0.001$) and negative correlation. Because these parameters are poorly understood for soft-bodied ticks, future research is needed to biologically quantify these parameters.

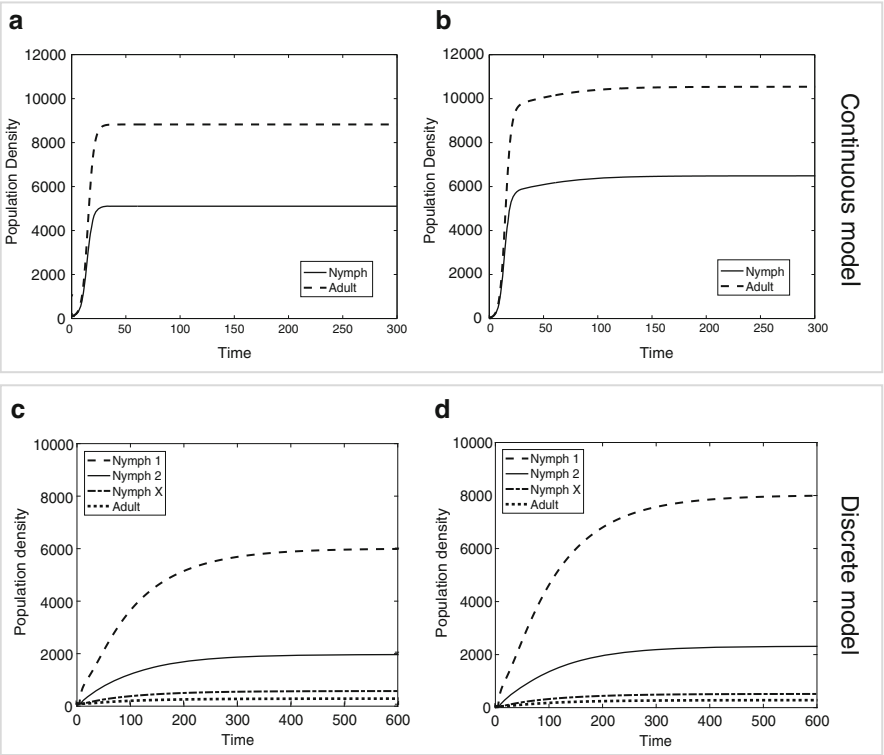

Fig. 2 (**a**)–(**b**) Simulated tick density per life stage over time using the continuous-time model with baseline parameters in Tables 1 and 2 and initial tick density N(0) = 70, and A(0) =0. (**c**)–(**d**) Simulated tick density per stage over time using the discrete-time model with baseline parameter values in Tables 4 and 5 and initial tick density $\mathbf{T}(0) = \text{col}(70, 0, 0, 0)$. For all graphs, small hosts are assumed to be at carrying capacity with 1 small host/hectare ($S(0) = 1$). In graphs (**a**) and (**c**), no large hosts are present ($L(0) = 0$). In graphs (**b**) and (**d**), large hosts are introduced ($L(0) = 0.01$) and increase to carrying capacity (0.025 large host/hectare)

5 Discrete-Time Model

In this section, we develop a discrete-time, structured population model for the soft tick feeding on two types of hosts, small hosts S and large hosts L. As with the continuous-time model, the host densities can be thought of as constant or time-dependent. For non-constant host densities, if we assume that the host populations are independent of each other as well as the tick population, we can describe the populations according to

$$S(t+1) = r_S \frac{1}{1 + k_S S(t)} S(t), \tag{5.1}$$

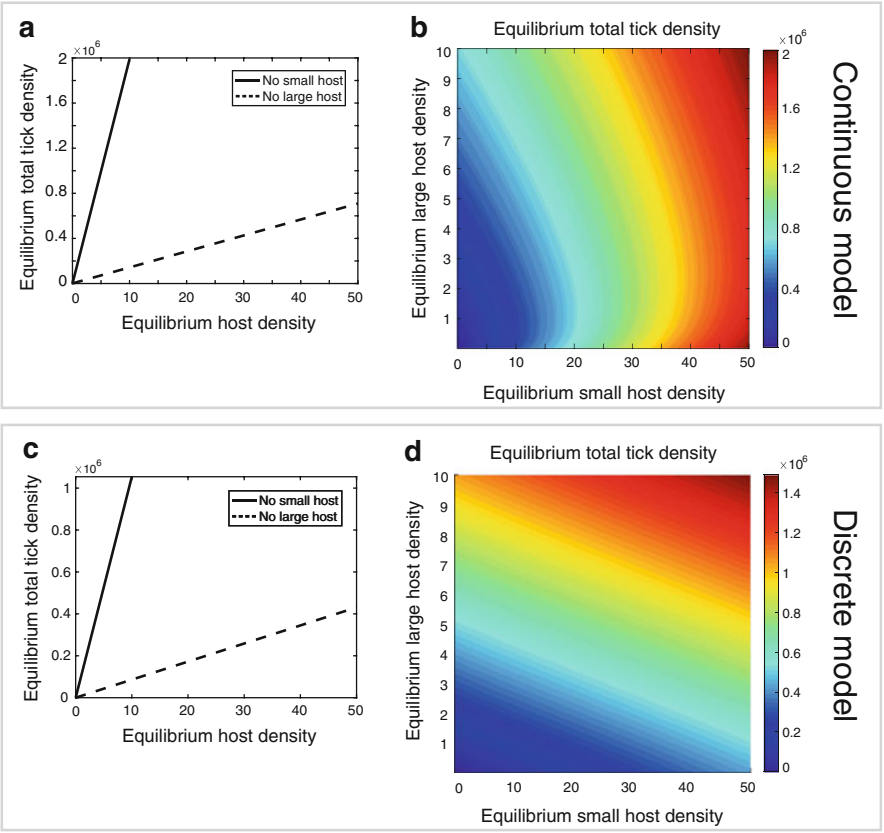

Fig. 3 Equilibrium total tick density as a function of equilibrium small and large host densities for the continuous-time model (**a**)–(**b**) and the discrete-time model (**c**)–(**d**). Parameters are selected from baselines in Tables 1 and 2 for the continuous-time model and baselines from Tables 4 and 5 for the discrete-time model. (**a**) Total tick density increases approximately linearly with no small host (solid black line) or with no large host (dashed black line). Eliminating only one host will not drive the ticks to extinction. (**b**) Total tick density using the continuous-time model when both large and small hosts are present. (**c**) Total tick density increases approximately linearly with small host density if there are no large hosts and with large host density if there are no small hosts. Note that eliminating either host without the other will not drive the ticks to extinction in this case. (**d**) Total tick density using the discrete-time model when both large and small hosts are present

$$L(t+1) = r_L \frac{1}{1 + k_L L(t)} L(t), \tag{5.2}$$

where r_S and r_L are the growth expansion factors of hosts S and L, respectively, and k_S and k_L are intraspecific competition coefficients. Table 4 provides parameter values, ranges, and units for the host populations. We note that these values were chosen so that the host equilibrium values are the same as those in the continuous-time model.

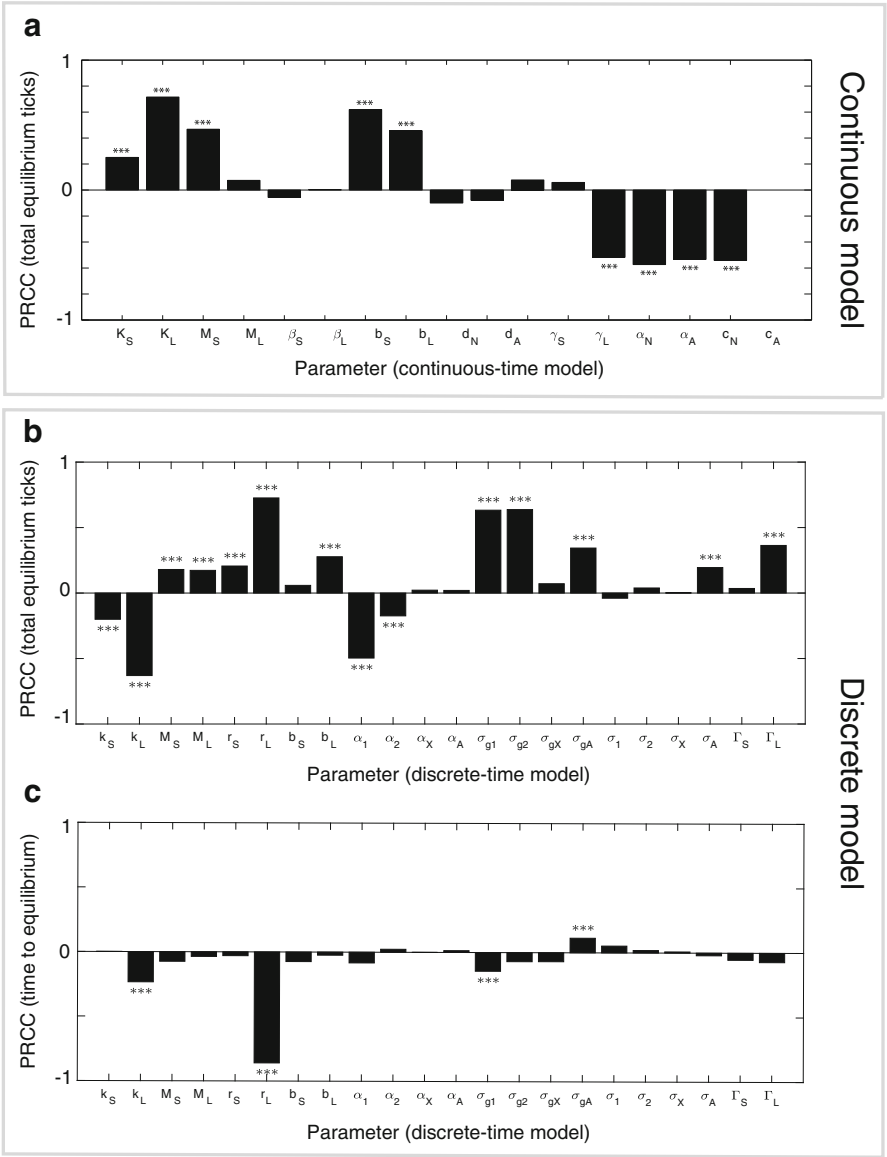

Fig. 4 Sensitivity and uncertainty analysis using Latin hypercube sampling (LHS) of parameter space and partial rank correlation coefficients (PRCC). (**a**) PRCC of equilibrium total tick density in the continuous-time model. (**b**) PRCC of equilibrium total tick density in the discrete-time model. (**c**) PRCC of time to reach within 0.01 of the equilibrium density in the discrete-time model (initial condition $\mathbf{T}(0) = \text{col}(70, 0, 0, 0)$). All parameter ranges for the continuous-time model are given in Tables 1 and 2. All parameter ranges for the discrete-time model are given in Tables 4 and 5. A total of 1000 simulations were executed to obtain all PRCC values. *** indicates significance ($p < 0.001$)

Table 4 Variables and parameters for host populations for the discrete-time model

Variable	Description	Units			
S	Density of small host	[hosts/ha]			
L	Density of large host	[hosts/ha]			
Parameter	Description	Units	Range	Baseline	Citations(s)
k_S	Intraspecific competition for host S	[ha/hosts]	(0.08, 2)	0.2	[8, 33]
k_L	Intraspecific competition for host L	[ha/hosts]	(0.02, 0.2)	2.4	[22]
r_S	Average expansion factor for host S	Unitless	(1.02, 5)	1.2	[8, 32]
r_L	Average expansion factor of host L	Unitless	(1.002, 1.2)	1.06	[7]

Area is measured in hectares ($100\,m^2$). Time is measured in 2-week intervals

The aim of this model is to capture some of the aspects of the life history of soft ticks that are not captured by the two-stage nymph-adult continuous-time model presented in the previous section. As with the continuous-time model, we assume host-specific fecundity in which the large host is the more beneficial host. We also incorporate two additional biological aspects of the soft tick life cycle. First, we assume that the blood meal obtained from a large host is better quality resulting in fewer nymph stages, but the probability of reaching maturity in the minimum number of instars is the same for feeding on both types of hosts. As a result, transition probabilities following a meal on a large host are larger than transition probabilities following a meal on a small host. Second, it is possible that nymphs will be interrupted while feeding or will have an insufficient amount of energy necessary to molt [17]. If this occurs, they will require a second meal to complete their molt. We represent this in the models as feeding but not transitioning. Feeding without transitioning has the effect of "resetting" the biological clock, allowing a tick to remain in the same stage for a longer amount of time. We therefore assume that survival rates are dependent upon whether a tick that feeds transitions to the next stage.

We describe the soft tick life cycle using four stages: three nymph stages N_1, N_2, N_X and one adult stage A. This simplification of the soft tick life cycle is obtained by combining the first and second nymph classes into N_1 and the third through fifth nymph classes into N_2. Movement between the stages is described in Fig. 1b. It is possible for an individual nymph to bypass the third nymph stage, N_X, provided that in stage N_2 it receives a sufficiently large blood meal from a large host. Meanwhile, the second nymph stage, N_2, ensures that first-stage nymphs, N_1, cannot immediately reach maturity.

We describe the dynamics of the soft tick population by the system

$$\begin{aligned}
N_1(t+1) &= \sigma_{s_1}(S(t), L(t), \mathbf{T}(t))N_1(t) + \beta(S(t), L(t), \mathbf{T}(t))A(t),\\
N_2(t+1) &= \sigma_{g_1}\gamma_1(S(t), L(t), \mathbf{T}(t))N_1(t) + \sigma_{s_2}(S(t), L(t), \mathbf{T}(t))N_2(t),\\
N_X(t+1) &= \sigma_{g_2}\gamma_{2,S} f_{2,S}(S(t), L(t), \mathbf{T}(t))N_2(t) + \sigma_{s_X}(S(t), L(t), \mathbf{T}(t))N_X(t),\\
A(t+1) &= \sigma_{g_2}\gamma_{2,L} f_{2,L}(S(t), L(t), \mathbf{T}(t))N_2(t)\\
&\quad + \sigma_{g_X}\gamma_X(S(t), L(t), \mathbf{T}(t))N_X(t) + \sigma_{s_A}(S(t), L(t), \mathbf{T}(t))A(t),
\end{aligned} \tag{5.3}$$

where $\mathbf{T} = \text{col}(N_1, N_2, N_X, A)$ is the column vector containing the densities of the four stages. Here, we take the unit of time to be 2 weeks to accurately represent the maximum *O. moubata* nymph molting potential. This is also the minimum time between adult reproductive events [17].

Since life history processes for ticks depend upon obtaining blood meals, we define feeding functions $f_{i,S}$ and $f_{i,L}$, which give the fraction of stage i ticks that consume a meal from S or L hosts. This fraction is assumed to depend on the total number of meals available (without preference for a particular host) and is modified by interference from other ticks according to

$$f_{i,S}(S, L, \mathbf{T}) = \frac{M_S S}{\sum_j \alpha_{ij} T_j + M_S S + M_L L}, \tag{5.4}$$

$$f_{i,L}(S, L, \mathbf{T}) = \frac{M_L L}{\sum_j \alpha_{ij} T_j + M_S S + M_L L}, i = 1, 2, X, A. \tag{5.5}$$

Because more than one tick may feed on the same host, M_S and M_L give the number of blood meals provided by small and large hosts, respectively. Meanwhile, parameter α_{ij} gives the interference stage i experiences from stage j. We assume that $\alpha_{ij} \geq 1$ to ensure that the number of meals consumed does not exceed the number of meals available. By this choice for feeding functions, as the number of available meals grows large, the number of meals consumed approaches the total number of ticks present.

Birth and transition out of stage i are assumed to require a blood meal and thus depend upon the feeding functions according to

$$\beta(S, L, \mathbf{T}) = b_S f_{A,S}(S, L, \mathbf{T}) + b_L f_{A,L}(S, L, \mathbf{T}),$$
$$\gamma_i(S, L, \mathbf{T}) = \gamma_{i,S} f_{i,S}(S, L, \mathbf{T}) + \gamma_{i,L} f_{i,L}(S, L, \mathbf{T}), \ i = 1, 2, X.$$

Parameters b_S and b_L give the fecundity of an adult that has fed on a small or large host, respectively, while $\gamma_{i,S}$ and $\gamma_{i,L}$ give the probability of transitioning out of the i-th stage given a meal on a small or large host. The transition probability for a given stage will depend on the number of biological instars contained in that stage. We assume that stage N_2 nymphs transition to stage N_X nymphs if they obtain a meal from a small host (low quality), while N_2 nymphs transition to the adult stage if they receive a meal from a large host (high quality). However, this modeling assumption can be relaxed by allowing transitions to either stage to depend on meals from both hosts.

All nymphs of stage i survive to the next time unit with probability σ_{g_i}, which factors in the length of time that a nymph can remain in stage i without feeding. We assume no mortality occurs as a result of transitioning, and therefore nymphs that feed and transition have the same survival probability as those that do not feed. However, in the case that a nymph feeds without transitioning, it can remain in the stage longer, resulting in a boost in survivorship to σ_i. Therefore, for the nymph

stages, the probability of surviving and transitioning out of stage i is $\sigma_{g_i}\gamma_i$, while the probability of surviving and remaining in stage i is

$$\begin{aligned}\sigma_{s_i}(S,L,\mathbf{T}) = \sigma_i[(1-\gamma_{i,S})f_{i,S}(S,L,\mathbf{T}) + (1-\gamma_{i,L})f_{i,L}(S,L,\mathbf{T})] \\ + \sigma_{g_i}(1 - f_{i,S}(S,L,\mathbf{T}) - f_{i,L}(S,L,\mathbf{T})), \quad i = 1,2,X,\end{aligned}$$

where $\sigma_{g_i} \leq \sigma_i \leq 1$. The first term of σ_{s_i} gives the probability that a tick survives and feeds but does not transition. Meanwhile, the second term in σ_{s_i} is the probability that a tick survives but does not feed. If it is assumed that the only advantage to feeding is transitioning; that is, if $\sigma_i = \sigma_{g_i}$, then $\sigma_{s_i}(S,L,\mathbf{T})$ reduces to $\sigma_{g_i}(1-\gamma_i(S,L,\mathbf{T}))$. To define the survival of adult ticks, we note that individuals only leave the adult stage through death. In addition, since feeding results in reproduction and an adult female can only lay up to three clutches in her lifetime after which she dies [17], we assume that feeding shortens the amount of time spent in the adult stage, resulting in a lower survival probability for adults. Therefore, we define

$$\begin{aligned}\sigma_{s_A}(S,L,\mathbf{T}) = \sigma_A[f_{A,S}(S,L,\mathbf{T}) + f_{A,L}(S,L,\mathbf{T})] \\ + \sigma_{g_A}(1 - f_{A,S}(S,L,\mathbf{T}) - f_{A,L}(S,L,\mathbf{T})),\end{aligned}$$

where $\sigma_A \leq \sigma_{g_A}$ accounts for the fact that females have a limited number of reproductive events.

Table 5 summarizes the various variables, functions, and parameters as well as the units and parameter ranges for tick population.

5.1 Numerical Simulations

We examine the tick population dynamics analytically in Appendix. In particular, we determine a threshold value for tick persistence that is a function of large and small host densities. This threshold value is given by the inherent net reproductive number

$$R_0(S,L) = \frac{\beta\gamma_1\sigma_{g_1}\sigma_{g_2}\left(\gamma_{2,L}f_{2,L}(1-\sigma_{s_X}) + \gamma_{2,S}f_{2,S}\sigma_{g_X}\gamma_X\right)}{(1-\sigma_{s_1})(1-\sigma_{s_2})(1-\sigma_{s_X})(1-\sigma_{s_A})}, \tag{5.6}$$

where the functional dependencies have been dropped to simplify notation and all functions are evaluated at $(S,L,\mathbf{0})$. We show that if $R_0(S,L) < 1$, then the tick population goes extinct, while if $R_0(S,L) > 1$, the tick population is persistent.

We explore the effects of host density on the tick population by numerically simulating the discrete-time model (5.3). Unless otherwise indicated, we assume that small hosts, S, are constantly supplied at their carrying capacity of $(r_S - 1)/k_S = 1$ small host per hectare. For our simulations, we use the baseline

Table 5 Variables and parameters for the tick population for the discrete-time model

Variable	Description	Units			
N_1	Density of first nymph stage (immature)	[ticks/ha]			
N_2	Density of second nymph stage (can mature)	[ticks/ha]			
N_X	Density of third nymph stage (can mature)	[ticks/ha]			
A	Density of adult ticks	[ticks/ha]			
Function	Description	Units	Range		
$f_{i,S}(S, L, \mathbf{T})$	Feeding on host S by stage i	Unitless	(0, 1)		
$f_{i,L}(S, L, \mathbf{T})$	Feeding on host L by stage i	Unitless	(0, 1)		
$\beta(S, L, \mathbf{T})$	Number of N_1 nymphs from a single female clutch	Unitless	(0, 300)		
$\sigma_{s_i}(S, L, \mathbf{T})$	Survivorship of stage i assuming no transition	Unitless	(0, 1)		
$\gamma_i(S, L, \mathbf{T})$	Transition probability from stage i	Unitless	(0, 1)		
Parameter	Description	Units	Range	Baseline	Cit.
M_S	Number of meals per small host	[meals/tick]	(1200)	100	Estimated
M_L	Number of meals per large host	[meals/tick]	(400, 600)	500	Estimated
α_{ij}	Intraspecific interference of T_j on T_i	[meals/tick]	[1, 5]	1	Estimated
b_S	Number of N_1 nymphs from an adult female due to a meal from host S	Unitless	(20, 70)	70	[3, 5, 25]
b_L	Number of N_1 nymphs from an adult female due to a meal from host L	Unitless	(45, 230)	230	[3, 25]
Γ_L	Probability an N_1 nymph reaches A in 5 instars when feeding on host L	Unitless	(0, 1)	0.5	[25]
Γ_S	Probability an N_1 nymph reaches A in 6 instars when feeding on host S	Unitless	(0, 1)	0.5	[26]
$\gamma_{i,S}$	Transition probability for tick in stage i that has fed on host S	Unitless	(0, 1)	0.79, 0.71, 0.89	[25]
$\gamma_{i,L}$	Transition probability for tick in stage i that has fed on host L	Unitless	(0, 1)	0.76, 0.66, 0.87	[26]
σ_{g_i}	Baseline survival of stage i	Unitless	(0, 1)	0.98, 0.98, 0.98, 0.98	[17]
σ_i	Survival of stage i assuming feeding but not transitioning	Unitless	(0, 1)	0.99, 0.99, 0.99, 0.67	[17]

Area is measured in hectares (100 m^2); time is measured in 2-week intervals. Index $i = 1, 2, X, A$ unless otherwise indicated

parameters given in Tables 4 and 5 and assume that initially there exist only 70 stage-1 ticks per hectare ($N_1(0) = 70$ and $N_2(0) = N_X(0) = A(0) = 0$).

Figure 2c, d gives the time evolution of ticks in the four different stages when small hosts are at carrying capacity with no large hosts ($S(0) = 1,\ L(0) = 0$) versus when large hosts are introduced at a low level and increase to carrying capacity ($S(0) = 1,\ L(0) = 0.01$). Supplying a constant small host at carrying capacity each time unit results in around 8600 ticks per hectare in total at equilibrium, in comparison with approximately 11,200 ticks per hectare (or 1.3 times as many) when large hosts are present. This is due to the fact that the fecundity of adult ticks benefits more from large hosts compared with small hosts. Hence, the more large hosts that are present at each unit time, the greater the total tick density. Recall that ticks feeding on small hosts need one extra instar, N_X, to mature relative to those feeding on large hosts. Therefore, the presence of large hosts results in a shorter time to adulthood, thus "speeding up" the population dynamics. Specifically, while the time to equilibrium is longer when large hosts are present due to the higher tick equilibrium level, the average population growth rate (defined as the total tick density increase at equilibrium divided by the time for the population to reach 99% of the equilibrium) is shorter, as seen in Table 3. For instance, in Fig. 2, the average population growth rate increases by 28.61% when large hosts are introduced.

As with the continuous-time model, we investigate how the equilibrium of the total tick density changes with host density in Fig. 3c, d. We use the minimum and maximum carrying capacities to define the ranges for small hosts, [0.01, 50] hosts per hectare, and large hosts, [0.01, 10] hosts per hectare. The total tick equilibrium increases linearly with the number of small hosts when no large hosts are present, and vice versa. However, the rate of increase in the equilibrium level per large host is approximately 12 times that per small host. Figure 3d displays the influence of both small and large hosts on total tick density.

5.2 *Sensitivity Analysis*

We calculate partial rank correlation coefficient (PRCC) values in Fig. 4b, c to determine model sensitivity to individual parameters. To reduce the number of parameters, we make the simplifying assumption that the competitive effect of stage N_j on stage N_i is the same for all i; that is, we assume $a_j = a_{ij}$ for all i. To derive the transition probabilities $\gamma_{i,S}$ and $\gamma_{i,L}$ in Table 4, we assume probabilities of a stage N_1 nymph reaching the adult class A in six or five instars when feeding on a small or large host, respectively, and an equal probability of transitioning between instars. We denote these probabilities by the parameters Γ_S and Γ_L.

From Fig. 4b, we observe that the equilibrium total tick density is most sensitive to large host intraspecific competition and growth (k_L and r_L), baseline survivorship of young nymphs (σ_{g_1} and σ_{g_2}), and the ability of young nymphs to compete for meals (α_1). Since increasing either k_L or k_S decreases host density, these parameters are negatively correlated with total tick density. From Fig. 4c, we note the time to

reach the equilibrium total tick value is sensitive to parameters r_L and k_L, which determine total large host density. It is also sensitive to the survival of adult and stage N_1 nymphs (σ_{g_1} and σ_{g_A}). If we assume a different initial condition for the tick population, then these sensitivities may change. Specifically, if we consider the cases where all individuals start in any one of the four stages, then the time to equilibrium continues to be sensitive to r_L and k_L but its sensitivity to the survival probabilities σ_{g_i} may change.

6 Discussion

Comparing model results in Fig. 3 and Table 3, we observe that the two models predict similar equilibrium densities. However, while the equilibrium total tick densities in both models are comparable, it takes approximately four times longer for the discrete-time model to reach the equilibrium (that is, within 1% of the equilibrium value) compared to the stabilizing time for the continuous-time model. This is because the dynamics in the discrete-time model are slowed down by the extra stages in the soft tick life cycle. Specifically, in the continuous-time model, it is possible for a young tick to reach maturity in 1 week, while in the discrete-time model, it requires a minimum of 4 or 6 weeks for newly emerged nymphal ticks feeding on large or small hosts, respectively, to progress to adults. The discrete-time model results in larger values of R_0, the net reproductive number, with the difference increasing for increased host densities. In particular, when only small hosts are present and at carrying capacity, at low tick populations an adult tick produces 20% more new ticks in the discrete-time model. Meanwhile, if both hosts are present and at carrying capacity, then an adult tick produces 25% more new ticks. Since the continuous-time model predicts higher tick densities, this suggests that the effect of intraspecific competition is greater in the discrete-time model. Furthermore, the models agree that R_0, the net reproductive number, is greater than 1.0 even when only small hosts are present. This implies that once these ticks are introduced, the population will persist.

Little empirical data is available for soft ticks. Specifically, parameter estimates for the majority of tick-host dynamics have not been measured in laboratory or field experiments, and it is unclear if the data from tick life history lab experiments can be applied directly to field conditions. Therefore, from the PRCC values provided in Fig. 4, we can identify which life history parameters may be most important for predicting population dynamics and should be the focus of future laboratory or field studies. We observe that, for both models, tick density values are dependent upon parameters determining host densities and intraspecific competition. In addition, for the discrete-time model, tick density depends on certain survival rates and the transition term Γ_L. In general, we observe that tick density for the discrete-time model appears to be more correlated with properties related to the large host than the small host while the opposite is true for the continuous-time model.

7 Conclusions and Future Directions

The two models presented here are the first such models developed to explore the complex life history of soft ticks. One of the key findings through this effort is the large number of data gaps in the published literature for what is known about *O. moubata*, which is arguably one of the better studied soft tick species. These gaps are not surprising given the complexities of natural history and laboratory studies of species that can survive for many years without feeding and live up to 18 years. While the models vary in the time to equilibria, both models suggest that it is nearly impossible to eradicate these ticks in the presence of any suitable host. This raises the need for constant vigilance to prevent accidental introduction of *O. moubata* to new areas such as the USA [19].

These models are based on a soft tick, *Ornithodoros moubata*, that is of particular economic concern in Europe and Africa because it is a competent vector of African swine fever virus. The two models presented can now be extended to include the dynamics of this disease. Those models can then be used to explore both current and future control strategies. Additionally, the models have highlighted key biological data that need to be gathered and published for better parameterization as well as model validation. The models presented here are just the first steps in exploring the dynamics of these complex, yet important, disease vectors.

8 Data Availability

All software used to simulate and analyze the presented models is available from the corresponding author by request.

Acknowledgements The work described in this chapter was initiated during the Association for Women in Mathematics collaborative workshop Women Advancing Mathematical Biology hosted by the Mathematical Biosciences Institute (MBI) at Ohio State University in April 2017. Funding for the workshop was provided by MBI, NSF ADVANCE "Career Advancement for Women Through Research-Focused Networks" (NSF-HRD 1500481), Society for Mathematical Biology, and Microsoft Research.

Appendix

Model Analysis of Continuous-Time Model

First, we prove that the solutions of the continuous-time model (4.3) and (4.4) are well-posed.

THEOREM 1 *For any given* $N(0)$, $A(0) \geq 0$, *where both cannot be zero, the solutions of (4.3) and (4.4) are positive and bounded.*

Proof We first rewrite the model (4.3) and (4.4) as $\dot{N} = F_1(N, A)$ and $\dot{A} = F_2(N, A)$, and find that if $(N, A) \in \mathcal{R}^2_+ \cup (0, 0)$, then $F_1(0, A) \geq 0$ and $F_2(N, 0) \geq 0$. Then, we apply Theorem A.4 in [34], and prove that solutions of (4.3) and (4.4) are non-negative if the initial values are non-negative.

Next, for the boundedness, we let $(N, A) \in \mathcal{R}^2_+$, adding up (4.3) and (4.4) yields

$$\frac{\mathrm{d}\,(N + A)}{\mathrm{d}t} = (A_1 - A_8)A - A_4 N - A_2 N^2 - A_6 A^2 - (A_3 + A_7)NA. \tag{1}$$

It yields $\frac{\mathrm{d}(N+A)}{\mathrm{d}t} < 0$ with large positive values of N and A. Therefore, the value of $(N + A)$ is bounded. For notational simplicity, we denote parameters in model (4.3) and (4.4) as follows:

$$\begin{aligned} &A_1 = b_S\, S + b_L\, L, \quad A_2 = \tfrac{c_N}{M_S S + M_L L}, \quad A_3 = \alpha_N A_2, \quad A_4 = d_N, \\ &A_5 = \gamma_S S + \gamma_L L, \quad A_6 = \tfrac{c_A}{M_S S + M_L L}, \quad A_7 = A_6 \alpha_A, \quad A_8 = d_A. \end{aligned} \tag{2}$$

□

Therefore, we focus on the system (4.3) and (4.4), which yields one tick-free equilibrium $E_0 = (0, 0)$, and positive equilibrium: $E_1 = (\bar{N}, \bar{A})$. Then, for E_1, we have

$$\bar{N} = \frac{\bar{N}(A_6 \bar{A} + A_8)}{A_5 - A_7 \bar{A}}, \tag{3}$$

where $\bar{A}$ is determined by the following cubic equation:

$$F_1(\bar{A}) = C_0 \bar{A}^3 + C_1 \bar{A}^2 + C_2 \bar{A} + C_3. \tag{4}$$

Here, C_i are in terms of A_i parameters in (2), as follows:

$$\begin{aligned} C_0 &= A_6^2 A_2(\alpha_N \alpha_A - 1), \\ C_1 &= A_6 \left[(A_1 \alpha_A + A_4 + A_5) A_6 \alpha_2 - A_2(A_5 \alpha_N + A_8) + A_8 \frac{C_0}{A_6^2} \right], \\ C_2 &= -\frac{C_3 A_6 \alpha_A}{A_5} - A_2 A_8 (A_5 \alpha_N + A_8) - (A_1 \alpha_A + A_5 + A_4) A_5 A_6, \\ C_3 &= A_5(A_1 A_5 - A_4 A_8 - A_5 A_8). \end{aligned} \tag{5}$$

The local stability of the equilibrium solutions are determined by their corresponding eigenvalues solved from the corresponding characteristic polynomial as follows:

$$\begin{aligned} P(\lambda) &= \lambda^2 + B_1\lambda + B_2, \\ B_1 &= (2A_2 + A_7)\bar{N} + (A_3 + 2A_6)\bar{A} + A_4 + A_5 + A_8, \\ B_2 &= 4A_2A_6\bar{N}\bar{A} + 2A_2A_7\bar{N}^2 + 2A_3A_6\bar{A}^2 + (A_1A_7 + A_3A_8)\bar{A} \\ &\quad +(2A_2A_8 + A_3A_5)\bar{N}+(A_4 + A_5)(A_7\bar{N}+2A_6\bar{A})-A_1A_5+A_4A_8+A_5A_8 : \end{aligned} \tag{6}$$

Evaluating $P(\lambda)$ at E_0 yields

$$\begin{aligned} &P_0(\lambda) = \lambda^2 + B_{10}\lambda + B_{20}, \qquad \text{where,} \\ &B_{10} = A_4 + A_5 + A_8, \qquad B_{20} = -A_1A_5 + A_4A_8 + A_5A_8. \end{aligned} \tag{7}$$

THEOREM 2 *In original parameter values, we define a threshold as*

$$\begin{aligned} &B_{20} = -(Lb_L + Sb_S)(L\gamma_L + S\gamma_S) + (d_N + L\gamma_L + S\gamma_S)\, d_A \qquad \textit{or} \\ &R_0 = \frac{Lb_L + Sb_S}{d_A}\,\frac{1}{\frac{d_N}{L\gamma_L+S\gamma_S} + 1} \end{aligned} \tag{8}$$

- *when $B_{20} > 0$ or $R_0 < 1$, the tick-free equilibrium E_0 is locally asymptotically stable,*
- *when $B_{20} < 0$ or $R_0 > 1$, E_0 becomes unstable, while the positive equilibrium E_1 emerges,*
- *when $B_{20} = 0$ or $R_0 = 1$, a transcritical bifurcation occurs; moreover E_0 and E_1 intersect and exchange stability.*

Proof With all positive parameter values, the stability of E_0 is easily derived from $P_0(\lambda) = 0$ in (7). Since $C_3 = -A_5B_{20}$, we have $C_3 > 0$ and $C_2 < 0$, when $B_{20} < 0$. Therefore, the cubic equation (4) has at least one positive solution, denoted by E_1. Moreover, evaluating $P_0(\lambda) = 0$ at E_1 yields $B_2|_{E_1} = -B_{20}f_{E1}$, where f_{E1} is in terms of A_i parameters. Therefore, E_1 has one zero eigenvalue when $B_{20} = 0$. This proves the occurrence of the transcritical bifurcation. □

THEOREM 3 *With all positive parameter values and positive equilibrium solutions, no Hopf bifurcation occurs.*

Proof In (6), B_1 is always positive with positive solutions (N, A) and positive parameter values. Therefore, $B_1 = 0$ does not occur; thus, the necessary condition for a Hopf bifurcation is never satisfied for model (4.3)–(4.4). □

Model Analysis of Discrete-Time Model

In this section we examine the dynamics of the discrete-time model (5.3) assuming constant host densities. Model (5.3) can be represented by the matrix equation

$$\mathbf{T}(t+1) = P(S(t), L(t), \mathbf{T}(t))\mathbf{T}(t),$$

where the projection matrix $P(S, L, \mathbf{T})$ is given by

$$\begin{pmatrix} \sigma_{s_1}(S,L,\mathbf{T}) & 0 & 0 & \beta(S,L,\mathbf{T}) \\ \sigma_{g_1}\gamma_1(S,L,\mathbf{T}) & \sigma_{s_2}(S,L,\mathbf{T}) & 0 & 0 \\ 0 & \sigma_{g_2}\gamma_{2,S}f_{2,S}(S,L,\mathbf{T}) & \sigma_{s_X}(S,L,\mathbf{T}) & 0 \\ 0 & \sigma_{g_2}\gamma_{2,L}f_{2,L}(S,L,\mathbf{T}) & \sigma_{g_X}\gamma_X(S,L,\mathbf{T}) & \sigma_{s_A}(S,L,\mathbf{T}) \end{pmatrix}. \tag{9}$$

By the linearization principle [12], the extinction equilibrium $\mathbf{T} = \mathbf{0}$ is stable when the dominant eigenvalue of the inherent projection matrix $P(S, L, \mathbf{0})$ is less than 1 and unstable when it is greater than 1. Since the dominant eigenvalue and the inherent net reproductive number R_0 are on the same side of 1 [10], the same is true in terms of R_0.

The inherent net reproductive number of model (5.3) is given by

$$R_0(S,L) = \frac{\beta\gamma_1\sigma_{g_1}\sigma_{g_2}\left(\gamma_{2,L}f_{2,L}(1-\sigma_{s_X}) + \gamma_{2,S}f_{2,S}\sigma_{g_X}\gamma_X\right)}{(1-\sigma_{s_1})(1-\sigma_{s_2})(1-\sigma_{s_X})(1-\sigma_{s_A})},$$

where the functional dependencies have been dropped to simplify notation and all functions are evaluated at $(S, L, \mathbf{0})$. This value is defined to be the dominant eigenvalue of the matrix $F(I-U)^{-1}$, where F and U are obtained by decomposing the projection matrix (9) into a fertility matrix F and a transition matrix U, so that $P = F + U$ [10]. Theorem 4 establishes the condition for tick persistence and characterizes the behavior of model (5.3) in a neighborhood of $R_0 \approx 1$.

THEOREM 4 *Assume S and L are constant.*

(a) The extinction equilibrium $\mathbf{T} = \mathbf{0}$ is globally asymptotically stable for $R_0(S, L) < 1$.

(b) For $R_0(S, L) > 1$, the extinction equilibrium is unstable and system (5.3) is permanent; that is, there exists a positive constant $\delta > 0$ such that

$$\delta \le \lim_{t\to\infty} \inf |\mathbf{T}(t)| \le \lim_{t\to\infty} \sup |\mathbf{T}(t)| \le \frac{1}{\delta}$$

for all solutions $\mathbf{T}(t)$ satisfying $\mathbf{T}(0) \in R_+^4$ and $|\mathbf{T}(0)| > 0$.

(c) For $R_0(S, L) > 1$, a branch of positive equilibria bifurcates from the extinction equilibria. The positive equilibria are locally asymptotically stable in the neighborhood of $R_0(S, L) \gtrapprox 1$.

Proof

(a) By Theorem 1.1.3 of [10], R_0 and the dominant eigenvalue of $P(S, L, \mathbf{0})$ are on the same side of 1. Since the feeding functions (5.4) are decreasing functions of tick density, $P(S, L, \mathbf{T}) \leq P(S, L, \mathbf{0})$ holds for all $\mathbf{T} \in R_+^4$. Therefore, by Theorem 1.2.1 of [10], the extinction equilibrium is globally asymptotically stable for $R_0(S, L) < 1$.

(b) Assume $R_0(S, L) > 1$, then by Theorem B2 of [21], system (5.3) is permanent if it is dissipative. Since all nonzero entries of projection matrix P are decreasing functions of tick density, there exists a $K > 0$ such that for $|\mathbf{T}| > K$, the sum of each row of P is less than 1, that is, $\sum_i p_{ij}(S, L, \mathbf{T}) < 1$. By Theorem B1 of [21], system (5.3) is dissipative.

(c) By Theorem 1.2.5 of [10], a branch of positive equilibria bifurcates from the extinction equilibrium at $R_0(S, L) = 1$. Since projection matrix P contains only negative tick density effects, the bifurcation is forward; that is, the positive equilibria exist for $R_0(S, L) \gtrapprox 1$. Since the bifurcation is forward, by Theorem 1.2.6 of [10], the equilibria are stable in a neighborhood of $R_0(S, L) \gtrapprox 1$. □

References

1. A. Aeschlimann, T. Freyvogel, Biology and distribution of ticks of medical importance, in *Handbook of Clinical toxicology of Animal Venoms and Poisons*, ed. by J. Meier, J. White, vol. 236 (CRC Press, Boca Raton, 1995), pp. 177–189
2. S.A. Allan, Ticks (Class Arachnida: Order Acarina), in *Parasitic Diseases of Wild Mammals*, 2nd edn. (Iowa State University Press, Ames, 2001), pp. 72–106
3. D.A. Apanaskevich, J.H. Oliver Jr., Life cycles and natural history of ticks. Biol. Ticks **1**, 59–73 (2014)
4. M. Arias, J.M. Sánchez-Vizcaíno, A. Morilla, K.-J. Yoon, J.J. Zimmerman, African swine fever, *Trends in Emerging Viral Infections of Swine* (Iowa State University Press, Ames, 2002), pp. 119–124
5. A. Astigarraga, A. Oleaga-Pérez, R. Pérez-Sánchez, J.A. Baranda, A. Encinas-Grandes, Host immune response evasion strategies in Ornithodoros erraticus and O. moubata and their relationship to the development of an antiargasid vaccine. Parasite Immunol. **19**, 401–410 (1997)
6. S. Blome, C. Gabriel, M. Beer, Pathogenesis of African swine fever in domestic pigs and European wild boar. Virus Res. **173**, 122–130 (2013)
7. J. Boshe, Reproductive ecology of the warthog *Phacochoerus aethiopicus* and its significance for management in the Eastern Selous Game Reserve, Tanzania. Biol. Conserv. **20**, 37–44 (1981)
8. T. Clutton-Brock, A. Maccoll, P. Chadwick, D. Gaynor, R. Kansky, and J. Skinner, Reproduction and survival of suricates (*Suricata suricatta*) in the Southern Kalahari. Afr. J. Ecol. **37**, 69–80 (1999)
9. S. Costard, B. Wieland, W. De Glanville, F. Jori, R. Rowlands, W. Vosloo, F. Roger, D.U. Pfeiffer, L.K. Dixon, African swine fever: how can global spread be prevented? Philos. Trans. R. Soc. B Biol. Sci. **364**, 2683–2696 (2009)
10. J.M. Cushing, *An Introduction to Structured Population Dynamics* (SIAM, Philadelphia, 1998)

11. S.J. Cutler, A. Abdissa, J.-F. Trape, New concepts for the old challenge of African relapsing fever borreliosis. Clin. Microbiol. Infect. **15**, 400–406 (2009)
12. S. Elaydi, *An Introduction to Difference Equations* (Springer, Berlin, 2005)
13. H. Gaff, E. Schaefer, Metapopulation models in tick-borne disease transmission modelling, in *Modelling Parasite Transmission and Control* (Springer, Berlin, 2010), pp. 51–65
14. H.D. Gaff, L.J. Gross, Modeling tick-borne disease: a metapopulation model. Bull. Math. Biol. **69**, 265–288 (2007)
15. J.S. Gray, A. Estrada-Peña, L. Vial, Ecology of nidicolous ticks. Biol. Ticks **2**, 39–60 (2014)
16. W.R. Hess, African swine fever virus, in *African Swine Fever Virus* (Springer, Berlin, 1971), pp. 1–33
17. H. Hoogstraal, Argasid and nuttalliellid ticks as parasites and vectors. Adv. Parasitol. **24**, 135–238 (1985)
18. H. Hoogstraal, A. Aeschlimann, Tick-host specificity. Bull. de la société Entomologique Suisse **55**, 5–32 (1982)
19. J.E. Keirans, L.A. Durden, Invasion: exotic ticks (Acari: Argasidae, Ixodidae) imported into the United States. a review and new records. J. Med. Entomol. **38**, 850–861 (2001)
20. N. Keyfitz, *Introduction to the Mathematics of Population* (Addison-Wesley, Reading MA, 1968)
21. R. Kon, Y. Iwasa, Single-class orbits in nonlinear Leslie matrix models for semelparous populations. J. Math. Biol. **55**, 781–802 (2007)
22. J. Kruger, B. Reilly, I. Whyte, Application of distance sampling to estimate population densities of large herbivores in Kruger National Park. Wildl. Res. **35**, 371–376 (2008)
23. E.C. Loomis, Life histories of ticks under laboratory conditions (Acarina: Ixodidae and Argasidae). J. Parasitol. **47**, 91–99 (1961)
24. B. Lubisi, R. Dwarka, D. Meenowa, R. Jaumally, An investigation into the first outbreak of African swine fever in the Republic of Mauritius. Transbound. Emerg. Dis. **56**, 178–188 (2009)
25. C.K. Mango, R. Galun, Suitability of laboratory hosts for rearing of *Ornithodoros moubata* ticks (Acari: Argasidae). J. Med. Entomol. **14**, 305–308 (1977)
26. C.K. Mango, R. Galun, *Ornithodoros moubata*: breeding in vitro. Exp. Parasitol. **42**, 282–288 (1977)
27. S. Marino, I.B. Hogue, C.J. Ray, D.E. Kirschner, A methodology for performing global uncertainty and sensitivity analysis in systems biology. J. Theor. Biol. **254**, 178–196 (2008)
28. N. Meshkat, C. E.-Z. Kuo, J. DiStefano III, On finding and using identifiable parameter combinations in nonlinear dynamic systems biology models and COMBOS: a novel web implementation. PloS One **9**, e110261 (2014)
29. M.-L. Penrith, W. Vosloo, F. Jori, A.D. Bastos, African swine fever virus eradication in Africa. Virus Res. **173**, 228–246 (2013)
30. W. Plowright, J. Parker, M. Peirce, African swine fever virus in ticks (*Ornithodoros moubata*, Murray) collected from animal burrows in Tanzania. Nature **221**, 1071–1073 (1969)
31. J.M. Sánchez-Vizcaíno, L. Mur, B. Martínez-López, African swine fever: an epidemiological update. Transbound. Emerg. Dis. **59**, 27–35 (2012)
32. C. Schradin, N. Pillay, Demography of the striped mouse (*Rhabdomys pumilio*) in the succulent karoo. Mamm. Biology-Zeitschrift für Säugetierkunde **70**, 84–92 (2005)
33. C. Schradin, N. Pillay, Intraspecific variation in the spatial and social organization of the African striped mouse. J. Mammal. **86**, 99–107 (2005)
34. H.R. Thieme, *Mathematics in Population Biology* (Princeton University Press, Princeton, 2003)
35. T. Vergne, A. Gogin, D. Pfeiffer, Statistical exploration of local transmission routes for African swine fever in pigs in the Russian federation, 2007–2014. Transbound. Emerg. Dis. **64**, 504–512 (2017)
36. L. Vial, Biological and ecological characteristics of soft ticks (Ixodida: Argasidae) and their impact for predicting tick and associated disease distribution. Parasite **16**, 191–202 (2009)
37. E. Vinuela, African swine fever virus, in *Iridoviridae* (Springer, Berlin, 1985), pp. 151–170

Ami Radunskaya • Rebecca Segal • Blerta Shtylla
Editors

Understanding Complex Biological Systems with Mathematics

Springer

Editors
Ami Radunskaya
Mathematics Department
Pomona College
Claremont, CA, USA

Rebecca Segal
Department of Mathematics
Virginia Commonwealth University
Richmond, VA, USA

Blerta Shtylla
Mathematics Department
Pomona College
Claremont, CA, USA

ISSN 2364-5733 ISSN 2364-5741 (electronic)
Association for Women in Mathematics Series
ISBN 978-3-319-98082-9 ISBN 978-3-319-98083-6 (eBook)
https://doi.org/10.1007/978-3-319-98083-6

Library of Congress Control Number: 2018959746

Mathematics Subject Classification: 92-06, 92-B05

This Springer imprint is published by the registered company Springer Nature Switzerland AG
The registered company address is: Gewerbestrasse 11, 6330 Cham, Switzerland

Contents